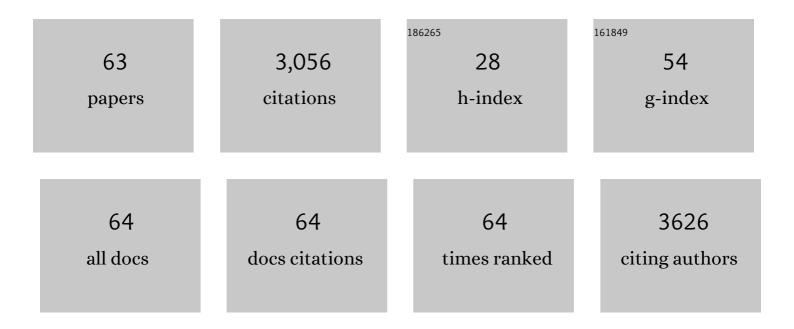
List of Publications by Year in descending order

Source: https://exaly.com/author-pdf/7929680/publications.pdf Version: 2024-02-01



#	Article	IF	CITATIONS
1	A review of carbon monitoring in wet carbon systems using remote sensing. Environmental Research Letters, 2022, 17, 025009.	5.2	29
2	Modeling the hydrologic effects of watershed-scale green roof implementation in the Pacific Northwest, United States. Journal of Environmental Management, 2021, 277, 111418.	7.8	23
3	Classifying Forest Type in the National Forest Inventory Context with Airborne Hyperspectral and Lidar Data. Remote Sensing, 2021, 13, 1863.	4.0	13
4	Estimating Fuel Moisture in Grasslands Using UAV-Mounted Infrared and Visible Light Sensors. Sensors, 2021, 21, 6350.	3.8	8
5	Characterizing spatiotemporal variations of forest canopy gaps using aerial laser scanning data. International Journal of Applied Earth Observation and Geoinformation, 2021, 104, 102588.	2.8	2
6	Quantifying fire trends in boreal forests with Landsat time series and self-organized criticality. Remote Sensing of Environment, 2020, 237, 111525.	11.0	24
7	Stratifying Forest Overstory for Improving Effective LAI Estimation Based on Aerial Imagery and Discrete Laser Scanning Data. Remote Sensing, 2020, 12, 2126.	4.0	5
8	Wetland Surface Water Detection from Multipath SAR Images Using Gaussian Process-Based Temporal Interpolation. Remote Sensing, 2020, 12, 1756.	4.0	8
9	Characterizing Tree Spatial Distribution Patterns Using Discrete Aerial Lidar Data. Remote Sensing, 2020, 12, 712.	4.0	12
10	Characterizing the Spatial Variations of Forest Sunlit and Shaded Components Using Discrete Aerial Lidar. Remote Sensing, 2020, 12, 1071.	4.0	8
11	Lidar-based approaches for estimating solar insolation in heavily forested streams. Hydrology and Earth System Sciences, 2019, 23, 2813-2822.	4.9	7
12	First-entry wildfires can create opening and tree clump patterns characteristic of resilient forests. Forest Ecology and Management, 2019, 454, 117659.	3.2	42
13	Relationships between Satellite-Based Spectral Burned Ratios and Terrestrial Laser Scanning. Forests, 2019, 10, 444.	2.1	9
14	Forest structure predictive of fisher (Pekania pennanti) dens exists in recently burned forest in Yosemite, California, USA. Forest Ecology and Management, 2019, 444, 174-186.	3.2	17
15	Accurate Ground Positioning Obtained From 3d Data Matching Between Airborne and Terrestrial Data for Ground Validation of Satellite Laser. , 2019, , .		2
16	Harnessing the Temporal Dimension to Improve Object-Based Image Analysis Classification of Wetlands. Remote Sensing, 2018, 10, 1467.	4.0	22
17	Population responses of common ravens to reintroduced gray wolves. Ecology and Evolution, 2018, 8, 11158-11168.	1.9	7
18	Mapping the Individual Trees in Urban Orchards by Incorporating Volunteered Geographic Information and Very High Resolution Optical Remotely Sensed Data: A Template Matching-Based Approach. Remote Sensing, 2018, 10, 1134.	4.0	20

#	Article	IF	CITATIONS
19	Retrieving forest canopy extinction coefficient from terrestrial and airborne lidar. Agricultural and Forest Meteorology, 2017, 236, 1-21.	4.8	31
20	Highâ€resolution habitat modeling with airborne LiDAR for red tree voles. Journal of Wildlife Management, 2017, 81, 58-72.	1.8	15
21	Retrieving Directional Gap Fraction, Extinction Coefficient, and Effective Leaf Area Index by Incorporating Scan Angle Information From Discrete Aerial Lidar Data. IEEE Transactions on Geoscience and Remote Sensing, 2017, 55, 577-590.	6.3	39
22	Urbanization Alters the Influence of Weather and an Index of Forest Productivity on Avian Community Richness and Guild Abundance in the Seattle Metropolitan Area. Frontiers in Ecology and Evolution, 2017, 5, .	2.2	5
23	Object-Based Tree Species Classification in Urban Ecosystems Using LiDAR and Hyperspectral Data. Forests, 2016, 7, 122.	2.1	52
24	An Integrated Approach for Monitoring Contemporary and Recruitable Large Woody Debris. Remote Sensing, 2016, 8, 778.	4.0	13
25	Determining woody-to-total area ratio using terrestrial laser scanning (TLS). Agricultural and Forest Meteorology, 2016, 228-229, 217-228.	4.8	32
26	Improved Salient Feature-Based Approach for Automatically Separating Photosynthetic and Nonphotosynthetic Components Within Terrestrial Lidar Point Cloud Data of Forest Canopies. IEEE Transactions on Geoscience and Remote Sensing, 2016, 54, 679-696.	6.3	80
27	Urban food crop production capacity and competition with the urban forest. Urban Forestry and Urban Greening, 2016, 15, 58-64.	5.3	21
28	Assessing the Contribution of Woody Materials to Forest Angular Gap Fraction and Effective Leaf Area Index Using Terrestrial Laser Scanning Data. IEEE Transactions on Geoscience and Remote Sensing, 2016, 54, 1475-1487.	6.3	35
29	Reconstructing semi-arid wetland surface water dynamics through spectral mixture analysis of a time series of Landsat satellite images (1984–2011). Remote Sensing of Environment, 2016, 177, 171-183.	11.0	105
30	Terrestrial Laser Scanning Reveals Seagrass Microhabitat Structure on a Tideflat. Remote Sensing, 2015, 7, 3037-3055.	4.0	10
31	Assessing the utility of green LiDAR for characterizing bathymetry of heavily forested narrow streams. Remote Sensing Letters, 2014, 5, 352-357.	1.4	8
32	LUMINATE: linking agricultural land use, local water quality and Gulf of Mexico hypoxia. European Review of Agricultural Economics, 2014, 41, 431-459.	3.1	41
33	Terrestrial Laser Scanning for Vegetation Sampling. Sensors, 2014, 14, 20304-20319.	3.8	17
34	Deriving pseudo-vertical waveforms from small-footprint full-waveform LiDAR data. Remote Sensing Letters, 2014, 5, 332-341.	1.4	28
35	Uncertainty in urban forest canopy assessment: Lessons from Seattle, WA, USA. Urban Forestry and Urban Greening, 2014, 13, 152-157.	5.3	37
36	Evaluation of the contribution of LiDAR data and postclassification procedures to object-based classification accuracy. Journal of Applied Remote Sensing, 2014, 8, 083529.	1.3	6

#	Article	IF	CITATIONS
37	Estimation of forest structure and canopy fuel parameters from small-footprint full-waveform LiDAR data. International Journal of Wildland Fire, 2014, 23, 224.	2.4	73
38	Retrieval of Effective Leaf Area Index in Heterogeneous Forests With Terrestrial Laser Scanning. IEEE Transactions on Geoscience and Remote Sensing, 2013, 51, 777-786.	6.3	93
39	Monitoring Post Disturbance Forest Regeneration with Hierarchical Object-Based Image Analysis. Forests, 2013, 4, 808-829.	2.1	4
40	Hyperspectral Analysis of Soil Nitrogen, Carbon, Carbonate, and Organic Matter Using Regression Trees. Sensors, 2012, 12, 10639-10658.	3.8	36
41	Computational-Geometry-Based Retrieval of Effective Leaf Area Index Using Terrestrial Laser Scanning. IEEE Transactions on Geoscience and Remote Sensing, 2012, 50, 3958-3969.	6.3	60
42	Spatial variability of terrestrial laser scanning based leaf area index. International Journal of Applied Earth Observation and Geoinformation, 2012, 19, 226-237.	2.8	23
43	Leaf Orientation Retrieval From Terrestrial Laser Scanning (TLS) Data. IEEE Transactions on Geoscience and Remote Sensing, 2012, 50, 3970-3979.	6.3	70
44	Retrieving Forest Inventory Variables with Terrestrial Laser Scanning (TLS) in Urban Heterogeneous Forest. Remote Sensing, 2012, 4, 1-20.	4.0	172
45	Tree Species Detection Accuracies Using Discrete Point Lidar and Airborne Waveform Lidar. Remote Sensing, 2012, 4, 377-403.	4.0	85
46	Monitoring Urban Tree Cover Using Object-Based Image Analysis and Public Domain Remotely Sensed Data. Remote Sensing, 2011, 3, 2243-2262.	4.0	84
47	Strengths and limitations of assessing forest density and spatial configuration with aerial LiDAR. Remote Sensing of Environment, 2011, 115, 2640-2651.	11.0	55
48	Object-based classification of semi-arid wetlands. Journal of Applied Remote Sensing, 2011, 5, 053511.	1.3	35
49	Fourier transformation of waveform Lidar for species recognition. Remote Sensing Letters, 2011, 2, 347-356.	1.4	14
50	Fusion of LiDAR and imagery for estimating forest canopy fuels. Remote Sensing of Environment, 2010, 114, 725-737.	11.0	207
51	Capturing tree crown formation through implicit surface reconstruction using airborne lidar data. Remote Sensing of Environment, 2009, 113, 1148-1162.	11.0	175
52	Modeling approaches to estimate effective leaf area index from aerial discrete-return LIDAR. Agricultural and Forest Meteorology, 2009, 149, 1152-1160.	4.8	198
53	Retrieving Leaf Area Index (LAI) Using Remote Sensing: Theories, Methods and Sensors. Sensors, 2009, 9, 2719-2745.	3.8	411
54	3D Visualization for the Analysis of Forest Cover Change. Geocarto International, 2004, 19, 103-112.	3.5	11

4

#	Article	IF	CITATIONS
55	Relationship between airborne multispectral image texture and aspen defoliation. International Journal of Remote Sensing, 2004, 25, 2701-2711.	2.9	25
56	Multiâ€layer Forest Stand Discrimination with Spatial Coâ€occurrence Texture Analysis of High Spatial Detail Airborne Imagery. Geocarto International, 2002, 17, 55-68.	3.5	14
57	Supervised Classification of Multisource Satellite Image Spectral and Texture Data for Agricultural Crop Mapping in Buenos Aires Province, Argentina. Canadian Journal of Remote Sensing, 2001, 27, 679-684.	2.4	7
58	Interpretation of Forest Harvest Conditions in New Brunswick Using Landsat TM Enhanced Wetness Difference Imagery (EWDI). Canadian Journal of Remote Sensing, 2001, 27, 118-128.	2.4	41
59	Quantification of landscape change from satellite remote sensing. Forestry Chronicle, 2000, 76, 877-886.	0.6	30
60	Interpretation and Classification of Partially Harvested Forest Stands in the Fundy Model Forest Using Multitemporal Landsat TM Digital Data. Canadian Journal of Remote Sensing, 2000, 26, 318-333.	2.4	53
61	Incorporating texture into classification of forest species composition from airborne multispectral images. International Journal of Remote Sensing, 2000, 21, 61-79.	2.9	244
62	An ARC/INFO Macro Language (AML) Polygon Update Program (PUP) Integrating Forest Inventory and Remotely-Sensed Data. Canadian Journal of Remote Sensing, 2000, 26, 566-575.	2.4	3
63	Temporal signatures and harmonic analysis of natural and anthropogenic disturbances of forested landscapes: a case study in the Yellowstone region. , 0, , .		0